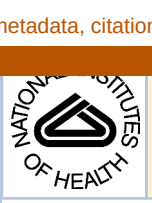

Published in final edited form as:
J Neurosurg. 2009 June ; 110(6): 1189–1197. doi:10.3171/2008.9.JNS08158.

Intravenous mesenchymal stem cell therapy for traumatic brain injury:

Laboratory investigation

Matthew T. Harting, M.D.[1], **Fernando Jimenez, M.S.**[1], **Hasan Xue, M.D.**[1], **Uwe M. Fischer, M.D.**[1], **James Baumgartner, M.D.**[1], **Pramod K. Dash, Ph.D.**[2,3], and **Charles S. Cox Jr., M.D.**[1]

[1]Departments of Pediatric Surgery, University of Texas Medical School at Houston, Texas

[2]Neurobiology and Anatomy, University of Texas Medical School at Houston, Texas

[3]The Vivian L. Smith Center for Neurologic Research, University of Texas Medical School at Houston, Texas

Abstract

Object—Cell therapy has shown preclinical promise in the treatment of many diseases, and its application is being translated to the clinical arena. Intravenous mesenchymal stem cell (MSC) therapy has been shown to improve functional recovery after traumatic brain injury (TBI). Herein, the authors report on their attempts to reproduce such observations, including detailed characterizations of the MSC population, non–bromodeoxyuridine-based cell labeling, macroscopic and microscopic cell tracking, quantification of cells traversing the pulmonary microvasculature, and well-validated measurement of motor and cognitive function recovery.

Methods—Rat MSCs were isolated, expanded in vitro, immunophenotyped, and labeled. Four million MSCs were intravenously infused into Sprague-Dawley rats 24 hours after receiving a moderate, unilateral controlled cortical impact TBI. Infrared macroscopic cell tracking was used to identify cell distribution. Immunohistochemical analysis of brain and lung tissues 48 hours and 2 weeks postinfusion revealed transplanted cells in these locations, and these cells were quantified. Intraarterial blood sampling and flow cytometry were used to quantify the number of transplanted cells reaching the arterial circulation. Motor and cognitive behavioral testing was performed to evaluate functional recovery.

Results—At 48 hours post-MSC infusion, the majority of cells were localized to the lungs. Between 1.5 and 3.7% of the infused cells were estimated to traverse the lungs and reach the arterial circulation, 0.295% reached the carotid artery, and a very small percentage reached the cerebral parenchyma (0.0005%) and remained there. Almost no cells were identified in the brain tissue at 2 weeks postinfusion. No motor or cognitive functional improvements in recovery were identified.

Conclusions—The intravenous infusion of MSCs appeared neither to result in significant acute or prolonged cerebral engraftment of cells nor to modify the recovery of motor or cognitive function. Less than 4% of the infused cells were likely to traverse the pulmonary microvasculature and reach

Address correspondence to: Charles S. Cox Jr., M.D., Department of Pediatric Surgery, University of Texas Medical School at Houston, 6431 Fannin Street, MSB 5.254, Houston, Texas 77030. charles.s.cox@uth.tmc.edu..

Disclosure

This work was supported by National Institutes of Health Grant Nos. T32 GM008792-06 (M.T.H.), MO1 RR 02558 (C.S.C.), and R21 HD 04 2659-01A1 (C.S.C.), as well as funds from the Children's Memorial Hermann Hospital Foundation (C.S.C.) and Texas Higher Education Coordinating Board (C.S.C.).

Disclaimer

The authors report no conflict of interest concerning the materials or methods used in this study or the findings specified in this paper.

the arterial circulation, a phenomenon termed the "pulmonary first-pass effect," which may limit the efficacy of this therapeutic approach. The data in this study contradict the findings of previous reports and highlight the potential shortcomings of acute, single-dose, intravenous MSC therapy for TBI.

Keywords

adult stem cell; cellular therapy; in vivo tracking; mesenchymal stem cell; traumatic brain injury

Cell therapy has garnered significant interest as a treatment strategy for a wide range of diseases over the last decade. Heart disease, peripheral vascular disease, bone disease, cancer, hepatic disease, and neurological disease have all been the focus of promising cell therapy breakthroughs.[7,15,23,24,34,40,48] Traumatic brain injury is one area in which positive preclinical evidence has led to the initiation of early clinical trials (www.clinicaltrials.gov).

Although cell therapy has been hailed as one of the next frontiers in modern medicine, there has been no universal agreement on many of the findings of early cell therapy work. Questions and concerns regarding many aspects of cell therapy, including transdifferentiation,[6,8,33,39,41,44] cell labeling,[5] route of administration,[37] preferred cell type, and immune privilege,[1,26,35] have been raised. Furthermore, publication bias may have skewed the expectations surrounding this treatment strategy.

Intravenous infusion has been used as the means of cell delivery in a large number of preclinical studies[16,19,27,32,43] as well as some early clinical trials.[14,17,21] Intravenous delivery has been asserted to be advantageous because of its broad distribution, ability to handle a large-volume infusion, and ease of access.[32] Nonetheless, questions have been raised regarding its ability to transport a critical number of cells to the area of injury.[28,37,42] Previous work has shown that cell infusion via the intravenous route allows a significant number of cells to reach the traumatically injured brain and to modulate significant functional recovery.[25,27,30,32]

We report on intravenously infused rat MSCs as therapy for TBI. We hypothesized that intravenously administered rat MSCs could reach the traumatically injured rat brain in critical numbers and improve the recovery of motor and cognitive function. We used well-characterized rat MSCs, non–BrdU-based cell labeling, and a CCI injury model. Behavioral outcomes were evaluated with well-validated measures of motor (rotarod, NSS, balance beam, and foot fault) and cognitive (Morris water maze, learning paradigm) function.

Methods

Isolation, Characterization, and Labeling of Rat MSCs

All protocols involving the use of animals were in compliance with the National Institutes of Health *Guide for the Care and Use of Laboratory Animals* and were approved by the Institutional Animal Care and Use Committee (protocols HSC-AWC-06–038, 07–055, and 07–113). Details of the rat MSC isolation and characterization techniques have been submitted for publication elsewhere. Briefly, we isolated MSCs from the bone marrow of Sprague-Dawley rats. We expanded the MSCs on a fibronectin matrix in multipotent adult progenitor cell medium.[4] Flow cytometric immunophenotyping was used to ensure that the MSCs were $CD11b^-$, $CD45^-$, $CD29^+$, $CD49e^+$, $CD73^+$, $CD90^+$, $CD105^+$, and Stro-1^+. Additionally, the multilineage potential was confirmed via differentiation to chondrocytes, adipocytes, and osteocytes. Cells between Passages 3 and 8 were used, because cells in earlier passages have not been found to be homogeneous and cells in later passages can change their phenotype and/or genotype. The MSCs were labeled with Qtracker 655 (immunohistochemistry and flow cytometry of intraarterial sampling) or Qtracker 800 (Odyssey infrared imaging) cell labeling kits (Invitrogen), according to the manufacturer's protocol. Cell labeling efficiency was > 90%.

Controlled Cortical Impact Injury

A CCI device (eCCI, model 6.3, Custom Design) was used to administer a unilateral brain injury, as described previously.[22] Rats were anesthetized with 4% isoflurane and a 1:1 mixture of N_2O/O_2, and the head of each animal was mounted in a stereotactic frame. The head was held in a horizontal plane, a midline incision was made for exposure, and a 7- to 8-mm craniectomy was performed on the right cranial vault. The center of the craniectomy was placed at the midpoint between the bregma and lambda, ~ 3 mm lateral to the midline, overlying the temporoparietal cortex. Using a 6-mm-diameter impactor tip, we delivered to each animal a single impact with a depth of deformation of 3.1 mm, an impact velocity of 6 m/second, and a dwell time of 150 msec (moderately severe injury) at an angle of 10° from the vertical plane, making the impact orthogonal to the surface of the cortex. An audible baseline monitor was used to ensure that the location of the tip relative to the surface of the brain was consistent prior to each impact. The blow was delivered to the parietal association cortex. Sham injury involved anesthetizing the animals, making the midline incision, and separating the skin, connective tissue, and aponeurosis from the cranium before closing the incision. Rat body temperature was maintained at 37°C with the use of a heating pad. Previously obtained serial arterial blood gases have shown that animals do not become hypoxic during this procedure.

Intravenous Administration of MSCs

Twenty-four hours after the CCI, rats were anesthetized with 4% isoflurane and O_2. The right internal jugular vein was exposed, and a silicone tubing catheter (inner diameter 0.635 mm, outer diameter 1.19 mm) was inserted. The MSCs were infused in 1 ml of PBS vehicle by using a 1-ml catheter flush to ensure that all cells were infused. Control rats were infused with 1 ml of PBS vehicle only. The catheter was removed, the incision closed, and the animal allowed to wake up. Animal respirations were closely monitored throughout the procedure and waking period.

Immunohistochemical Analysis of Brain and Lung Tissues

At 2 days and 2 weeks after the intravenous infusion of 4×10^6 rat MSCs, coronal brain sections were obtained for immunohistochemical analysis. After intraperitoneal ketamine injections, the thoracic cavity was opened and room temperature PBS was infused for 15 minutes via the left ventricle. The heart was spontaneously beating on initiation of the infusion, and the animals were simultaneously allowed to exsanguinate via a right atrium puncture. Cold 4% paraformaldehyde was then perfused for 15 minutes via the left ventricle. The brain was extracted and placed in 4% paraformaldehyde at 4°C for 24–48 hours. The brain was then embedded in 3% agarose, sectioned at 50 μm in the coronal plane by using a vibrating-blade microtome (Leica Microsystems), stained with DAPI (Invitrogen), and placed on a slide. Two members of the research team viewed 2 sections from the anterior penumbra, anterior injury, central injury, posterior injury, and posterior penumbra regions of each rat brain. The cells per coronal section were counted, and the counts were averaged and extrapolated to the entire injury area (8 mm) and the brain.

The lungs were extracted and placed in 10% formalin at 4°C for 24 hours. The pulmonary tissue was then paraffin embedded, sectioned at 8 μm in the coronal plane, mounted on slides, and stained with DAPI. All tissue sections were viewed on a Nikon inverted fluorescent microscope (model TE-2000-U).

Intravenous Cell Infusion With Intraarterial Sampling

Cells were labeled with Qtracker 655, and intravenous cannulation was achieved as described above. Intraarterial cannulation of the common carotid artery was achieved (same size catheter as that used in the intravenous infusions), with the tip of the catheter extending to the junction

of the brachiocephalic trunk and the aortic arch. Rats were heparinized at 100 U/kg (~ 25 U/rat). Control intraarterial samples were collected (250 μl/sample) prior to infusion. Cell infusion (4×10^6 MSCs in 1 ml of vehicle) was initiated with continual intraarterial sample collection until ~ 10 minutes after completing the infusion (~ 30 samples total, at 250 μl/sample).

Samples were then analyzed via flow cytometry (BD LSR II, BD Biosciences) to detect labeled cells reaching the arterial circulation. To accurately determine the number of cells reaching the arterial circulation, a standard curve was developed by adding known amounts of labeled MSCs (10^4, 5×10^4, 10^5, 5×10^5, and 10^6) to control blood samples of the same volume as the experimental samples (250 μl). Labeled cells were counted per 20,000 total events, and each control sample was run in triplicate. A standard curve was generated, and the resulting formula was used to determine the cell counts per experimental sample.

Infrared Macroscopic Cell Tracking

At 2 days and 2 weeks after cell infusion the rats were killed, and the lungs, kidney, spleen, and liver were collected. Tissues were placed on an Odyssey 2.1 infrared imaging system (LI-COR Biosciences) and were visualized (wavelength 800 nm, resolution 84 μm, focus offset 1 mm) to identify the presence of labeled cells. The integrated intensity of each lung was obtained by outlining the complete visualized lung and using the formula for integrated intensity: $a(\Sigma I_i - [\text{pixels} \times {}_B])$, where a is the area per pixel, ΣI_i is the sum of the intensities of all pixels, pixels is the total number of pixels, and ${}_B$ is the average intensity of the background.

Behavioral Training and Testing

All members of the research team involved in the behavioral testing were blinded to the experimental groups. Cells were intravenously infused 24 hours after the CCI injury. The optimal MSC dose is unknown, and therefore doses of 2 and 4×10^6 cells were tested. Rats were divided into 4 groups (6 rats/group): 1) sham injury + vehicle infusion, 2) CCI + vehicle infusion, 3) CCI + infusion of 2×10^6 MSCs, and 4) CCI + infusion of 4×10^6 MSCs.

Motor, Strength, and Reflex Tasks: Rotarod, NSS, Balance Beam, and Foot Fault—Beginning Day 1 after injury, an accelerating rotarod was used to measure motor balance and coordination. The rotarod consisted of a rotating spindle (diameter 10 cm). All animals were tested in 3 trials per day on Days 1, 4, 7, and 14 after TBI. The velocity of the rod was started at 15 rpm and was increased 3 rpm every 5 seconds. We recorded the maximum speed maintained prior to failure, that is, a fall or an inability to stay on top of the rod.

An NSS was determined on Days 1, 4, 7, and 14 after TBI. Points are assigned for alterations in motor function, behavior, and reflexes so that the maximal score of 14 represents severe neurological dysfunction, whereas a score of 0 indicates normal, intact neurological function. The indices that comprise the NSS have been described in detail elsewhere.[11,32]

The ability to maintain balance on a beam was assessed on Days 1, 4, 7, and 14 after TBI. Animals were placed on a 1.5-cm-wide beam for 60 seconds or until they fell. The animals completed 3 trials per day.

The ability to traverse chicken wire was also assessed on Days 1, 4, 7, and 14 after TBI. Animals were placed on a chicken wire path 10 cm wide by 5 ft long, and left rear foot faults were counted over 50 steps. Three trials per day were completed.

Cognitive Task: Morris Water Maze—Two weeks after injury, animals were tested in a hidden-platform learning paradigm11 version of the Morris water maze task.13,[36] Animals

were tested in 4 trials per day for 5 consecutive days. Each trial was initiated by placing the animal in 1 of 4 randomly chosen locations, facing the wall of the tank. Animals were allowed to search for the hidden platform for a period of 60 seconds. If an animal failed to find the platform, it was placed on the platform by the experimenter and was allowed to remain there for 30 seconds before being returned to a warming cage for 4 minutes between trials. For each trial, movement within the maze was monitored with a video camera linked to tracking software (Chromotrack, San Diego Instruments). Latency to the platform was calculated as the time necessary to locate the hidden platform. Using the tracking software, we also calculated the time spent in the area near the platform and the time spent circle swimming.

Statistical Analysis

Differences in lung integrated intensities between experimental and control animals were determined using a t-test. An additional ANOVA with a post hoc Dunnett test was used to calculate differences between each of the animals. Differences in behavioral testing were assessed using repeated measures ANOVA with a post hoc Tukey-Kramer test. All data are expressed as the means ± SEM.

Results

Cells Identified in the Brain via Immunohistochemistry

Immunohistochemistry revealed a paucity of cells in the brain. Two days after cell infusion, 20 ± 6.65 cells (0.0005 ± 0.00017%) were identified in the brain parenchyma. Fifty percent of these cells were identified in the injury or penumbral parenchyma, and 75% were found in the ipsilateral hemisphere. At 2 weeks postinfusion, only 1 cell was noted in the more than 150 sections examined from all 6 rats. No cells positive for Qtracker staining were identified in the brains of control animals.

Distribution of Infused Cells as Identified by Infrared Tracking

Infrared cell tracking 48 hours after infusion revealed that the primary location of the cells was the pulmonary tissue (Fig. 1). The integrated intensity of the control lungs was 0.03 ± 0.03, whereas that of the MSC-treated lungs was 2.15 ± 0.44 ($p = 0.003$, t-test). An ANOVA comparing all experimental and control lungs revealed a significant difference ($p = 0.037$), but post hoc Dunnett testing revealed no significant differences between experimental animals. No differences in integrated intensity were identified in the liver, kidney, or spleen. Infrared imaging of the brain—both as a complete organ and after sectioning—showed no detectable changes in fluorescent or integrated intensity (images and analysis not shown). Immunohistochemistry confirmed scores of cells in the pulmonary microvasculature (Fig. 2).

Infrared cell tracking 2 weeks after infusion revealed that the number of cells remaining in the pulmonary tissue had decreased (Fig. 3). The integrated intensity of the control lungs was 0.66 ± 0.30, whereas that of the MSC-treated lungs was 1.29 ± 0.04 ($p = 0.10$, t-test). Again, no differences in integrated intensity were identified in the liver, kidney, or spleen.

Intravenous Infusion With Intraarterial Sampling

Regular arterial rat blood and Qtracker-labeled rat MSCs analyzed using flow cytometry are shown in Fig. 4A and B, respectively. More than 95% of labeled cells were Qtracker positive (a fluorescent intensity > 10^2 at a 655-nm wavelength), and 100% of whole blood cells were Qtracker negative (fluorescent intensity < 10^2). Therefore, we were able to establish a fluorescent intensity threshold of 10^2 for selecting positive cells from arterial sampling. Examples of MSCs counted when 100,000 and 10,000 cells were added to a control sample of blood are shown in Fig. 4C and D, respectively.

Positive controls were used to generate a standard curve with the following linear formula: MSC count = (39.86 × cells detected). This formula was used to estimate the number of cells reaching the arterial circulation. A mean of 11,800 ± 5,865 total cells (0.295 ± 0.112%) were found to reach the carotid arterial circulation. The majority of cells that did traverse the pulmonary circulation reached the arterial circulation within 5 minutes after infusion (Fig. 5).

Behavioral Assessment: Motor, Strength, and Reflex Tasks

No significant improvements were seen in the rotarod (Fig. 6), NSS, balance beam, or foot fault tests.

Behavioral Assessment: Cognitive Function

No significant improvement was seen on the Morris water maze (learning paradigm). Average latencies are shown in Table 1.

Discussion

Our data revealed that a single intravenous dose of 4×10^6 MSCs delivered 24 hours after a moderate TBI did not result in substantial cell engraftment or improved functional recovery. The majority of cells were localized to pulmonary tissue. We found that 0.295% of the cells traversed the pulmonary circulation and reached the right carotid artery, and only a very small subset (0.0005%) of the total number of cells actually reached the brain and remained there for 2 days. Of the cells that did reach the cerebral parenchyma, 50% were located in the area of direct injury and the penumbral area. There was no motor or cognitive function recovery benefit among rats receiving these cells.

Previous studies have shown greater numbers of intravenously infused MSCs reaching and remaining in the rodent brain after TBI, as well as some measure of functional recovery.[25,27,29-32] Although our overall experimental designs were similar, there are some key differences between the studies. Lu et al.25 and Mahmood et al.[32] used rat MSCs isolated after 10 days of culture and passaged only once. We found that a population of homogeneous (> 99%) MSCs cannot be obtained until Passage 3, so we used the MSCs after Passage 3. Our population of rat MSCs was immunocharacterized, differentiated, and from between Passages 3 and 8. Such detailed characterization is critical when comparing studies (or cell populations), but this assertion does not mean that our population of cells is optimal for reaching the brain or mitigating the behavioral deficits of a TBI. It is certainly possible that first-passage bone marrow cells (a mixture of mesenchymal and hematopoietic cells), such as those used by other authors,[25,29,32] are the preferred cell mixture. Additionally, cell passage may lead to phenotypic changes that alter the likelihood that a cell will be able to traverse the pulmonary microvasculature. Finally, authors of some previous studies have used BrdU to label or track cells.25 Given our concerns regarding the transfer of the BrdU label to native cells,[5] we labeled the cells in our study with the Qtracker labeling system. It is plausible that differences in cell populations and/or cell labeling are responsible for the observed data differences between previous studies and the present study.

Although few cells were noted in the rat brain, 50% of the identified cells appeared in the area of injury or the penumbral area. This finding is consistent with previously collected data showing greater cell numbers in the area of injury.[32] Local disruption of the blood-brain barrier, along with various mechanisms of homing to areas of inflammation such as the upregulation of cell adhesion molecules,[9] may be responsible for this phenomenon.

In addition, we chose a moderate CCI injury model. Although it is similar to the model commonly applied in previous studies of intravenous MSC infusion after TBI (although others

have used slightly less impact depth or bilateral craniotomies with unilateral injury), the degree of injury may be important in cell survival, as recent work has revealed that transplanted neural stem cells may survive better after mild TBI than after severe TBI.[38]

Our attempt to quantify the number of cells reaching the arterial circulation has some limitations. Physiological cardiac output in rats is ~ 25 ml/minute (range 10–60 ml/minute). With the catheter at the junction of the brachiocephalic trunk and the aortic arch, our arterial collection rate ranged from 2–5 ml/minute, or 8–20% of the total cardiac output. Given our observation that 0.295% of the infused cells were retrieved via the intraarterial catheter, 1.48–3.69% of the total cells infused may reach the entire arterial circulation. Because the brain also receives blood via the vertebral artery, slightly more than 0.295% of the cells may be reaching the brain. An additional limitation of this intraarterial sampling method is that it likely misses small numbers of cells that traverse the microvasculature over time. Even 48 hours after delivery, however, numerous cells remain in the lung, and so it is unlikely that we are missing a significant number of cells.

Cell trapping in the pulmonary microvasculature is at least partially related to cell size. Schrepfer and colleagues[37] have found that very few 4-μm microspheres are trapped by the lung, whereas 10- and 15-μm microspheres are trapped at rates ~ 20 and ~ 30 times greater, respectively. They also found mouse MSCs range from 15–19 μm and noted ~ 70 times more cells trapped in the lung, relative to the 4-μm microspheres. Interestingly, these authors noted significant decreases in the rates of microsphere and MSC trapping with vasodilator treatment. Forward-scatter flow cytometric analysis of our results revealed that the cells that do traverse the lungs are on the small end of the size spectrum (analysis not shown).

Although we have shown the limitations of a single intravenous dose of 4×10^6 rat MSCs in a moderate TBI model in rodents, we believe our findings are relevant to any disease model in which intravenous cell therapy is being investigated. The intravenous route is being used for cell delivery in preclinical work outside of TBI, including, but not limited to, cardiac disease,[45] peripheral neuropathy,[16] muscular dystrophy,[18] amyotrophic lateral sclerosis,[12] liver disease,[20] and Kaposi sarcoma.[15] The intravenous route is also being used in the treatment of pulmonary diseases such as bleomycin-induced lung injury[47] and lung tumors.[46]

Comparisons of cell delivery routes of have shown the intravenous method to be suboptimal, relative to other options. Barbash and colleagues[2] have compared the intravenous distribution with left ventricular MSC infusion and found limited general engraftment with the intravenous route due to pulmonary entrapment. Freyman and coworkers[10] have compared intravenous with intracoronary or endocardial MSC delivery in a porcine myocardial infarction model. They also noted increased myocardial engraftment with the intracoronary and endocardial route, as opposed to the intravenous route. They did caution that intracoronary delivery hampers coronary blood flow. Even multipotent adult progenitor cells, a smaller, multipotent bone marrow–derived progenitor cell type, were found to concentrate in the lung after intravenous infusion.[42] Bentzon et al.[3] have demonstrated that MSCs can be efficiently and nonspecifically trapped in the general microvasculature.

Eight clinical trials utilizing the intravenous cell delivery route are currently underway (www.clinicaltrials.gov). The target disorders include cirrhosis, diabetes, multiple sclerosis, myasthenia gravis, peripheral vascular disease, and TBI. More trials are being generated based on the overwhelming majority of promising preclinical results with cell delivery via this route. The pulmonary first-pass effect with intravenous cell delivery must be considered when designing such trials. As ongoing research seeks a critical cell number necessary for the repair of specific diseases or tissues, investigative efforts should be forged to minimize the pulmonary

first-pass effect—perhaps increased cell delivery, small cell selection, alteration of adhesion markers, rheological agent use, or pulmonary vasodilation.

Conclusions

We showed that a single intravenous dose of 4×10^6 MSCs delivered 24 hours after a moderate TBI does not lead to substantial cell engraftment or improved functional recovery. This result is largely attributable to the pulmonary first-pass effect, in which the pulmonary microvasculature denies significant cell passage into the arterial circulation. We estimate that only 1.48–3.69% of infused cells reach the arterial circulation, only 0.295% reach the right carotid artery, and only 0.0005% reach and remain in the traumatically injured brain. An accurate and complete understanding of the strengths and weaknesses of intravenous cell delivery is paramount to maximizing the cell therapy delivery strategy.

Abbreviations used in this paper

ANOVA	analysis of variance
BrdU	bromodeoxyuridine
CCI	controlled cortical impact
MSC	mesenchymal stem cell
NSS	neurological severity score
PBS	phosphate-buffered saline
TBI	traumatic brain injury

References

1. Badillo AT, Beggs KJ, Javazon EH, Tebbets JC, Flake AW. Murine bone marrow stromal progenitor cells elicit an in vivo cellular and humoral alloimmune response. Biol Blood Marrow Transplant 2007;13:412–422. [PubMed: 17382248]
2. Barbash IM, Chouraqui P, Baron J, Feinberg MS, Etzion S, Tessone A, et al. Systemic delivery of bone marrow-derived mesenchymal stem cells to the infarcted myocardium: feasibility, cell migration, and body distribution. Circulation 2003;108:863–868. [PubMed: 12900340]
3. Bentzon JF, Stenderup K, Hansen FD, Schroder HD, Abdallah BM, Jensen TG, et al. Tissue distribution and engraftment of human mesenchymal stem cells immortalized by human telomerase reverse transcriptase gene. Biochem Biophys Res Commun 2005;330:633–640. [PubMed: 15809044]
4. Breyer A, Estharabadi N, Oki M, Ulloa F, Nelson-Holte M, Lien L, et al. Multipotent adult progenitor cell isolation and culture procedures. Exp Hematol 2006;34:1596–1601. [PubMed: 17046581]
5. Burns TC, Ortiz-Gonzalez XR, Gutierrez-Perez M, Keene CD, Sharda R, Demorest ZL, et al. Thymidine analogs are transferred from prelabeled donor to host cells in the central nervous system after transplantation: a word of caution. Stem Cells 2006;24:1121–1127. [PubMed: 16373692]
6. Castro RF, Jackson KA, Goodell MA, Robertson CS, Liu H, Shine HD. Failure of bone marrow cells to transdifferentiate into neural cells in vivo. Science 2002;297:1299. [PubMed: 12193778]
7. Chamberlain JR, Schwarze U, Wang PR, Hirata RK, Hankenson KD, Pace JM, et al. Gene targeting in stem cells from individuals with osteogenesis imperfecta. Science 2004;303:1198–1201. [PubMed: 14976317]
8. English D, Klasko SK, Sanberg PR. Elusive mechanisms of “stem cell”-mediated repair of cerebral damage. Exp Neurol 2006;199:10–15. [PubMed: 16730352]
9. Fang J, Hall BK. Differential expression of neural cell adhesion molecule (NCAM) during osteogenesis and secondary chondrogenesis in the embryonic chick. Int J Dev Biol 1995;39:519–528. [PubMed: 7577443]

10. Freyman T, Polin G, Osman H, Crary J, Lu M, Cheng L, et al. A quantitative, randomized study evaluating three methods of mesenchymal stem cell delivery following myocardial infarction. Eur Heart J 2006;27:1114–1122. [PubMed: 16510464]
11. Fujimoto ST, Longhi L, Saatman KE, Conte V, Stocchetti N, McIntosh TK. Motor and cognitive function evaluation following experimental traumatic brain injury. Neurosci Biobe-hav Rev 2004;28:365–378.
12. Garbuzova-Davis S, Willing AE, Zigova T, Saporta S, Justen EB, Lane JC, et al. Intravenous administration of human umbilical cord blood cells in a mouse model of amyotrophic lateral sclerosis: distribution, migration, and differentiation. J Hematother Stem Cell Res 2003;12:255–270. [PubMed: 12857367]
13. Guzowski JF, McGaugh JL. Antisense oligodeoxynucleotide-mediated disruption of hippocampal cAMP response element binding protein levels impairs consolidation of memory for water maze training. Proc Natl Acad Sci U S A 1997;94:2693–2698. [PubMed: 9122258]
14. Horwitz EM, Prockop DJ, Fitzpatrick LA, Koo WW, Gordon PL, Neel M, et al. Transplantability and therapeutic effects of bone marrow-derived mesenchymal cells in children with osteogenesis imperfecta. Nat Med 1999;5:309–313. [PubMed: 10086387]
15. Khakoo AY, Pati S, Anderson SA, Reid W, Elshal MF, Rovira II, et al. Human mesenchymal stem cells exert potent antitumorigenic effects in a model of Kaposi's sarcoma. J Exp Med 2006;203:1235–1247. [PubMed: 16636132]
16. Klass M, Gavrikov V, Drury D, Stewart B, Hunter S, Denson DD, et al. Intravenous mononuclear marrow cells reverse neuropathic pain from experimental mononeuropathy. Anesth Analg 2007;104:944–948. [PubMed: 17377111]
17. Koc ON, Gerson SL, Cooper BW, Dyhouse SM, Haynesworth SE, Caplan AI, et al. Rapid hematopoietic recovery after coinfusion of autologous-blood stem cells and culture-expanded marrow mesenchymal stem cells in advanced breast cancer patients receiving high-dose chemotherapy. J Clin Oncol 2000;18:307–316. [PubMed: 10637244]
18. Kong KY, Ren J, Kraus M, Finklestein SP, Brown RH Jr. Human umbilical cord blood cells differentiate into muscle in sjl muscular dystrophy mice. Stem Cells 2004;22:981–993. [PubMed: 15536189]
19. Krause U, Harter C, Seckinger A, Wolf D, Reinhard A, Bea F, et al. Intravenous delivery of autologous mesenchymal stem cells limits infarct size and improves left ventricular function in the infarcted porcine heart. Stem Cells Dev 2007;16:31–37. [PubMed: 17348804]
20. Lagasse E, Connors H, Al-Dhalimy M, Reitsma M, Dohse M, Osborne L, et al. Purified hematopoietic stem cells can differentiate into hepatocytes in vivo. Nat Med 2000;6:1229–1234. [PubMed: 11062533]
21. Lazarus HM, Haynesworth SE, Gerson SL, Rosenthal NS, Caplan AI. Ex vivo expansion and subsequent infusion of human bone marrow-derived stromal progenitor cells (mesenchymal progenitor cells): implications for therapeutic use. Bone Marrow Transplant 1995;16:557–564. [PubMed: 8528172]
22. Lighthall JW. Controlled cortical impact: a new experimental brain injury model. J Neurotrauma 1988;5:1–15. [PubMed: 3193461]
23. Lorenzini S, Andreone P. Stem cell therapy for human liver cirrhosis: a cautious analysis of the results. Stem Cells 2007;25:2383–2384. [PubMed: 17540855]
24. Losordo DW, Dimmeler S. Therapeutic angiogenesis and vasculogenesis for ischemic disease: part II: cell-based therapies. Circulation 2004;109:2692–2697. [PubMed: 15184293]
25. Lu D, Mahmood A, Wang L, Li Y, Lu M, Chopp M. Adult bone marrow stromal cells administered intravenously to rats after traumatic brain injury migrate into brain and improve neurological outcome. Neuroreport 2001;12:559–563. [PubMed: 11234763]
26. Magliocca JF, Held IK, Odorico JS. Undifferentiated murine embryonic stem cells cannot induce portal tolerance but may possess immune privilege secondary to reduced major histocompatibility complex antigen expression. Stem Cells Dev 2006;15:707–717. [PubMed: 17105406]
27. Mahmood A, Lu D, Chopp M. Intravenous administration of marrow stromal cells (MSCs) increases the expression of growth factors in rat brain after traumatic brain injury. J Neurotrauma 2004;21:33–39. [PubMed: 14987463]

28. Mahmood A, Lu D, Chopp M. Marrow stromal cell transplantation after traumatic brain injury promotes cellular proliferation within the brain. Neurosurgery 2004;55:1185–1193. [PubMed: 15509325]
29. Mahmood A, Lu D, Lu M, Chopp M. Treatment of traumatic brain injury in adult rats with intravenous administration of human bone marrow stromal cells. Neurosurgery 2003;53:697–703. [PubMed: 12943585]
30. Mahmood A, Lu D, Qu C, Goussev A, Chopp M. Human marrow stromal cell treatment provides long-lasting benefit after traumatic brain injury in rats. Neurosurgery 2005;57:1026–1031. [PubMed: 16284572]
31. Mahmood A, Lu D, Qu C, Goussev A, Chopp M. Long-term recovery after bone marrow stromal cell treatment of traumatic brain injury in rats. J Neurosurg 2006;104:272–277. [PubMed: 16509501]
32. Mahmood A, Lu D, Wang L, Li Y, Lu M, Chopp M. Treatment of traumatic brain injury in female rats with intravenous administration of bone marrow stromal cells. Neurosurgery 2001;49:1196–1204. [PubMed: 11846913]
33. Mezey E, Nagy A, Szalayova I, Key S, Bratincsak A, Baffi J, et al. Comment on “Failure of bone marrow cells to transdifferentiate into neural cells in vivo”. Science 2003;299:1184. [PubMed: 12595675]
34. Perin EC, Dohmann HF, Borojevic R, Silva SA, Sousa AL, Mesquita CT, et al. Transendocardial, autologous bone marrow cell transplantation for severe, chronic ischemic heart failure. Circulation 2003;107:2294–2302. [PubMed: 12707230]
35. Priddle H, Jones DR, Burridge PW, Patient R. Hematopoiesis from human embryonic stem cells: overcoming the immune barrier in stem cell therapies. Stem Cells 2006;24:815–824. [PubMed: 16306149]
36. Schenk F, Morris RG. Dissociation between components of spatial memory in rats after recovery from the effects of retrohippocampal lesions. Exp Brain Res 1985;58:11–28. [PubMed: 3987843]
37. Schrepfer S, Deuse T, Reichenspurner H, Fischbein MP, Robbins RC, Pelletier MP. Stem cell transplantation: the lung barrier. Transplant Proc 2007;39:573–576. [PubMed: 17362785]
38. Shindo T, Matsumoto Y, Wang Q, Kawai N, Tamiya T, Nagao S. Differences in the neuronal stem cells survival, neuronal differentiation and neurological improvement after transplantation of neural stem cells between mild and severe experimental traumatic brain injury. J Med Invest 2006;53:42–51. [PubMed: 16537995]
39. Song L, Tuan RS. Transdifferentiation potential of human mesenchymal stem cells derived from bone marrow. FASEB J 2004;18:980–982. [PubMed: 15084518]
40. Srivastava D, Ivey KN. Potential of stem-cell-based therapies for heart disease. Nature 2006;441:1097–1099. [PubMed: 16810246]
41. Theise ND, Krause DS, Sharkis S. Comment on “Little evidence for developmental plasticity of adult hematopoietic stem cells”. Science 2003;299:1317. [PubMed: 12610282]
42. Tolar J, O’Shaughnessy MJ, Panoskaltsis-Mortari A, McEl-murry RT, Bell S, Riddle M, et al. Host factors that impact the biodistribution and persistence of multipotent adult progenitor cells. Blood 2006;107:4182–4188. [PubMed: 16410448]
43. Ukai R, Honmou O, Harada K, Houkin K, Hamada H, Kocsis JD. Mesenchymal stem cells derived from peripheral blood protects against ischemia. J Neurotrauma 2007;24:508–520. [PubMed: 17402856]
44. Wagers AJ, Sherwood RI, Christensen JL, Weissman IL. Little evidence for developmental plasticity of adult hematopoietic stem cells. Science 2002;297:2256–2259. [PubMed: 12215650]
45. Wolf D, Reinhard A, Krause U, Seckinger A, Katus HA, Kuecherer H, et al. Stem cell therapy improves myocardial perfusion and cardiac synchronicity: new application for echocardiography. J Am Soc Echocardiogr 2007;20:512–520. [PubMed: 17484992]
46. Xin H, Kanehira M, Mizuguchi H, Hayakawa T, Kikuchi T, Nukiwa T, et al. Targeted delivery of CX3CL1 to multiple lung tumors by mesenchymal stem cells. Stem Cells 2007;25:1618–1626. [PubMed: 17412895]
47. Xu J, Woods CR, Mora AL, Joodi R, Brigham KL, Iyer S, et al. Prevention of endotoxin-induced systemic response by bone marrow-derived mesenchymal stem cells in mice. Am J Physiol Lung Cell Mol Physiol 2007;293:L131–L141. [PubMed: 17416739]

48. Ziv Y, Avidan H, Pluchino S, Martino G, Schwartz M. Synergy between immune cells and adult neural stem/progenitor cells promotes functional recovery from spinal cord injury. Proc Natl Acad Sci U S A 2006;103:13174–13179. [PubMed: 16938843]

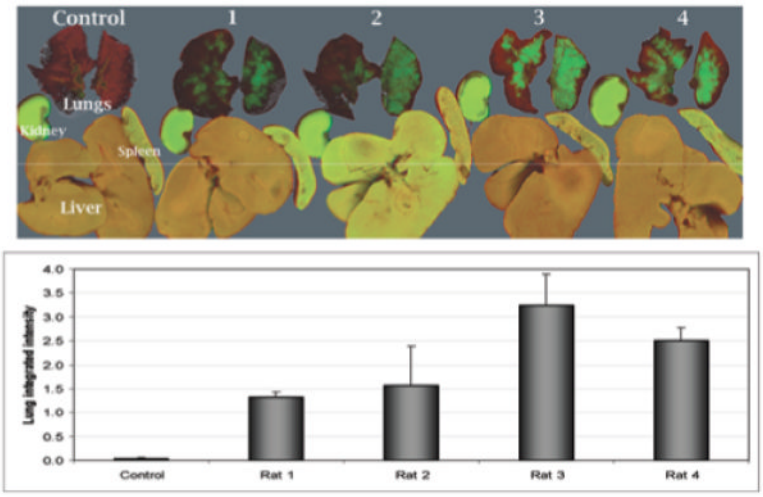

Fig. 1.

Upper: Infrared images (image resolution: 84 μm; focus offset: 1 mm) demonstrating intravenously infused MSCs in the lungs, kidney, spleen, and liver of rats 48 hours after the infusion of 4×10^6 MSCs (experimental rats 1–4) or PBS vehicle (Control). *Lower:* Bar graph showing the lung integrated intensities in the experimental animals, which were significantly different from those in controls ($p = 0.003$, t-test).

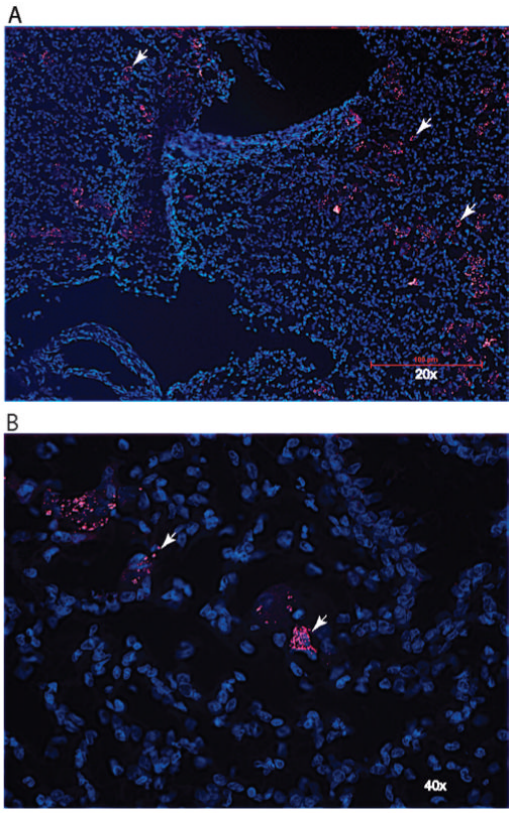

Fig. 2.

A and B: Photomicrographs showing numerous MSCs (Qtracker labeled) in the pulmonary tissue 48 hours after intravenous infusion. Cell nuclei are revealed by DAPI staining (blue) and MSCs by Qtracker 655 (red). *Arrowheads* indicate representative MSCs.

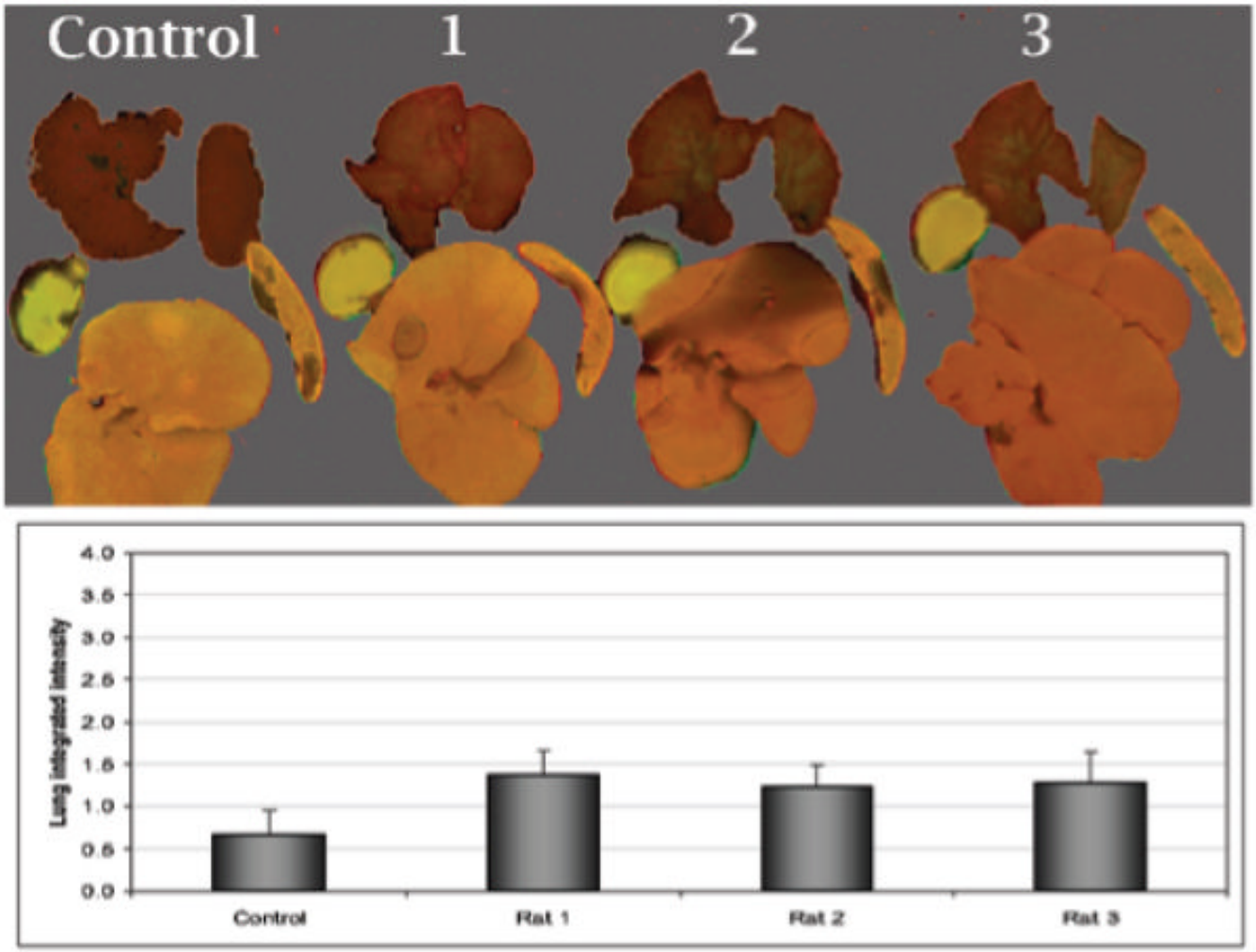

Fig. 3.

Upper: Infrared images (image resolution: 84 μm; focus offset: 1 mm) revealing the lungs, kidney, spleen, and liver of rats 2 weeks after the intravenous infusion of 4×10^6 MSCs (experimental rats 1–3) or vehicle (Control). Although some cells remain in the pulmonary tissue, there are significantly fewer than those seen 48 hours postinfusion. *Lower:* Bar graph showing lung integrated intensities of the experimental animals, which were not significantly different from those from controls ($p = 0.10$, t-test).

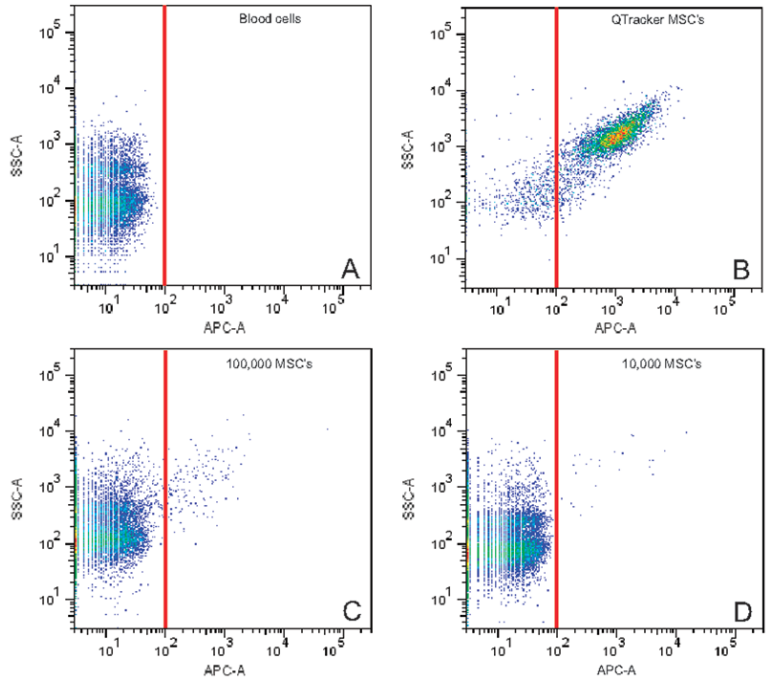

Fig. 4.

Flow cytometric scatterplot demonstrating rat whole blood cells (A) and Qtracker labeled rat MSCs (B). The red line shows the positive threshold (10^2) used to distinguish infused MSCs from other cells (> 95% of MSCs). The clear difference in intensity of rat blood (A) versus MSCs (B) allowed recognition of infused cells by flow cytometry. To generate a standard curve, MSC counts were obtained after adding known quantities of MSCs to control samples. Example scatterplots showing the effects of 100,000 MSCs (C) and 10,000 MSCs (D) added to control samples of rat blood. The number of cells with a fluorescent intensity > 10^2, after collecting 20,000 total events, was plotted against the known MSC number to generate the standard curve. APC-A = allophycocyanine–A channel; SSC-A = side scatter–A channel.

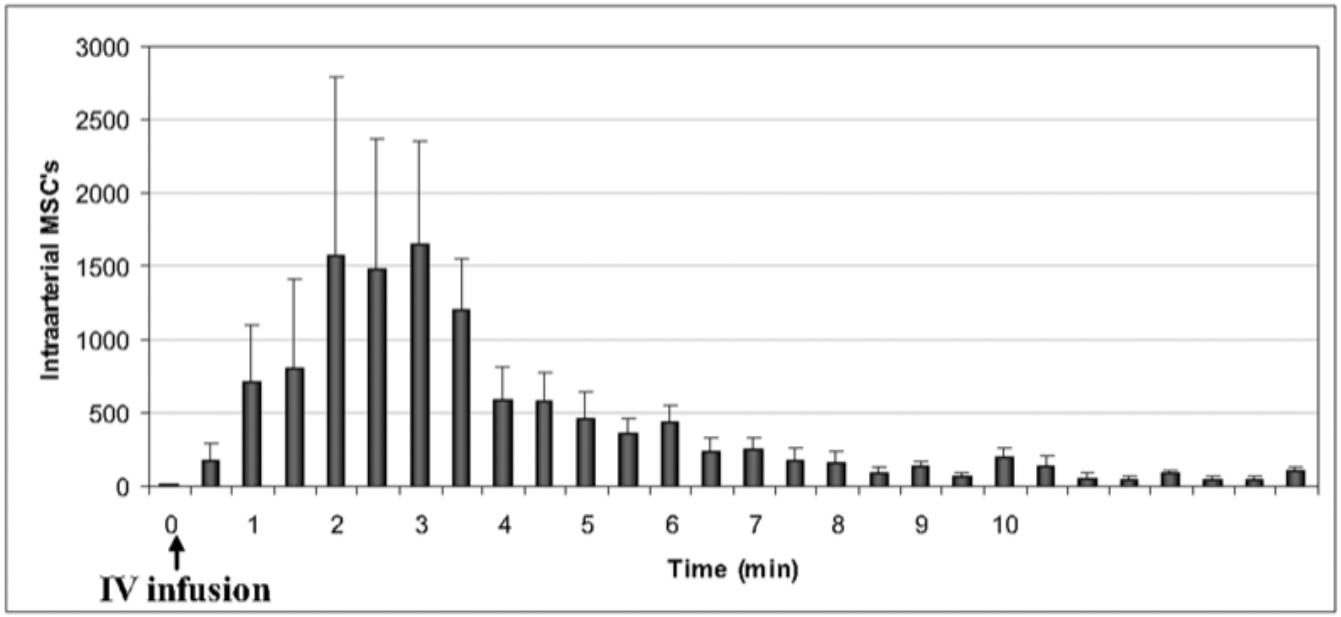

Fig. 5.

Bar graph showing Qtracker-labeled MSCs in intraarterial blood samples run through a flow cytometer. Four million rat MSCs (Qtracker labeled) were infused via the internal jugular vein (5 rats), and blood was continuously sampled from the common carotid artery over the subsequent 10 minutes. IV = intravenous.

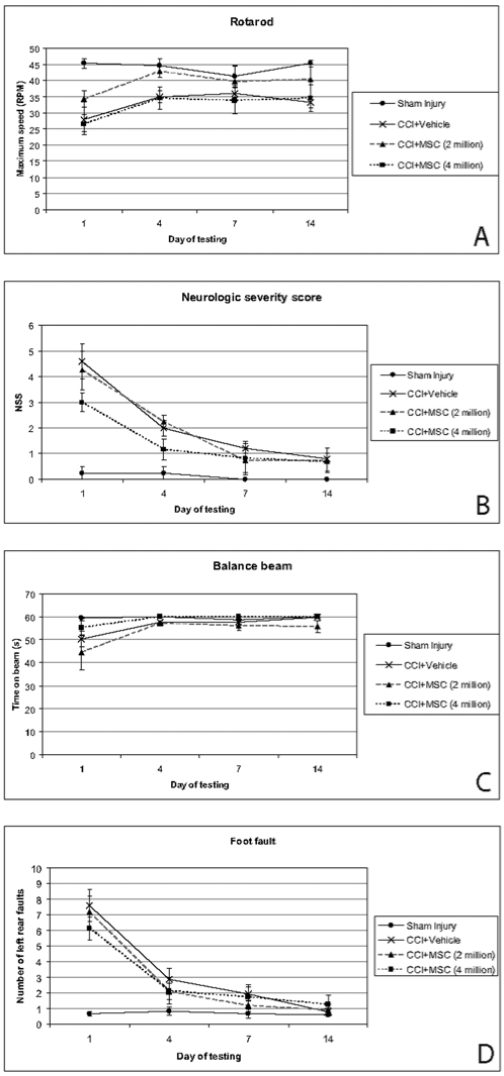

Fig. 6.

Graphs showing the results of rotarod (A), NSS (B), balance beam (C), and foot fault (D) testing. There were no significant differences between the CCI groups. Rotarod maximum speed is the highest rpm during which the rat could stay on the top of the rotating rod. Time on beam was measured from the time the animal was placed on the beam until the animal fell off and hit the safe landing area. Foot faults were counted when the left rear paw dropped below the chicken wire (out of 25 steps). Sham, 6 rats; CCI + vehicle, 5 rats; CCI + 2×10^6 MSCs, 4 rats; CCI + 4×10^6 MSCs, 6 rats. s = seconds.

TABLE 1

Morris water maze results in 21 rats*

Parameter	Sham Injury	CCI + Vehicle	CCI + 2 × 10^6 MSCs	CCI + 4 × 10^6 MSCs
no. of rats	6	5	4	6
testing day				
1	58.38 ± 1.1	57.51 ± 2.1	59.75 ± 0.1	57.03 ± 1.7
2	47.71 ± 5.6	57.12 ± 2.1	53.71 ± 3.5	44.68 ± 5.3
3	34.25 ± 5.1	48.36 ± 6.9	51.58 ± 7.7	41.87 ± 7.5
4	19.98 ± 4.2	51.10 ± 6.5	53.00 ± 5.7	54.45 ± 2.9
5	21.05 ± 4.1	40.06 ± 4.6	43.25 ± 4.5	38.88 ± 5.5

*Rats were tested in 4 trials per day (60 seconds maximum per trial) over 5 consecutive days. Results represent latency to the platform ± SEM in seconds. Latency to the platform is the time from placement of the animal in the water until it found the hidden platform. p = 0.441 (repeated measures ANOVA) in comparing the 3 CCI groups.

J Neurosurg. Author manuscript; available in PMC 2010 June 22.